Flag-based control of quantum purity for n=2 systems

Patrick Rooney, Anthony M. Bloch, and C. Rangan

Phys. Rev. A **93**, 063424 — Published 27 June 2016

DOI: 10.1103/PhysRevA.93.063424

Flag-based Control of Quantum Purity for $n = 2$ Systems

Patrick Rooney,* Anthony M. Bloch,[1,†] and C. Rangan[2,‡]

[1] *Department of Mathematics, University of Michigan, Ann Arbor, MI 48109*
[2] *Department of Physics, University of Windsor, ON, N9B 3P4, Canada*

This paper investigates the fast Hamiltonian control of $n = 2$ density operators by continuously varying the flag (*i.e.* the eigenspaces) as one moves away from the completely mixed state. In general, the critical points and zeros of the purity derivative can only be solved analytically in the limit of minimal purity. We derive differential equations that maintain these features as the purity increases. In particular, there is a thread of points in the Bloch ball that locally maximizes the purity derivative, and a corresponding thread that minimizes it. Additionally, we show there is a closed surface of points inside of which the purity derivative is positive, and inside of which is negative. We argue that this approach may be useful in studying higher-dimensional systems.

Keywords: quantum control, open systems, Lindblad equation, decoherence, dissipation

I. INTRODUCTION

In the last three decades, there has been great interest in controlling quantum systems for the purposes of coherent control of chemical reactions [1][2], NMR [3], and quantum computation [4][5]. One of the key challenges of quantum control is counter-acting the influence of the environment, which causes decoherence (loss of coherence between quantum states) and dissipation (loss of energy) (see [6], [7], [8] and [9] for surveys). If one models an open system as Markovian and time-independent, the dynamics are described by a quantum dynamical semigroup and the Lindblad master equation [10][11][12]. While there is research towards engineering open system dynamics[13][14][15], control functions often appear in the system Hamiltonian, which are only capable of steering within a given unitary orbit [16][17][18]. The motion *between* orbits depends on the Lindblad super-operator. This includes, in particular, variation in the purity $Tr(\rho^2)$, which is constant on any given orbit. This incentivizes unitary control that is fast relative to the time-scale of the Lindblad dynamics[19].

One method of representing open systems is the generalized Bloch representation [18][20], which yields an affine differential equation on the vector space of density operators. In this paper we use a different approach in which the structure of the space of density operators is decomposed into the space of unitary orbits, and the orbit manifolds themselves, which are complex flag manifolds [21][22]. If one has sufficiently fast and complete Hamiltonian control for an $n = 2$ system, the inter- and intra-orbit dynamics can be turned into a control equation, where the position along the orbit is considered a control variable, and the orbit itself is treated as a state variable [23][24]. Mathematically, the position along the orbit is a *flag*: a nesting of subspaces, which in this case are built out of the eigenspaces of the density operator. Our approach is based on continuously adjusting the eigenvectors, and thus we refer to our viewpoint as flag-based control. In a follow-up paper [26], we examine flag-based control for arbitrary $n > 2$ and how to approach the control of ρ by manipulating its flag.

The difficulty in this approach is that the orbit is a non-linear manifold, and applying standard control theory to obtain explicit trajectories is non-trivial. Controllability for $n = 2$ can be treated analytically, but not in a way that will scale practically to higher dimensions. At the completely mixed state however, the structure of the Lindblad term simplifies significantly regardless of dimension. This paper considers an approach that begins at the completely mixed state, and introduces a continuously varying adjustment in the flag, which maintains critical points and zeros of the purity derivative as the purity increases. In this way, one can plot a thread through ρ-space, the so-called Bloch ball, that maximizes (at least locally) the time-derivative of $Tr(\rho^2)$. There is a corresponding thread that minimizes the time-derivative (better said, maximizes it in the negative direction). Additionally, a different adjustment can be derived that maintains a surface that separates the Bloch ball into purity-increasing and purity-decreasing regions. The purity derivative on this surface vanishes.

We have not made any assumptions on the structure of the Lindblad super-operator. Dissipation of a two-level quantum system is often modelled with the phase-damping or amplitude-damping channels [25], which use simple Lindblad operators. In principle, there is no physical reason that more complicated channels could exist. Lindblad operators are obtained by tracing out the interaction of the system with the environment [12], and given the complexity of the environment, many different types of interactions may exist in nature. We have used a framework that describes generalized damping, where the Lindblad dissipation can be described by three phase-damping channels and a damping-bias vector. This framework incorporates the single phase-damping and amplitude-daming channels as particular cases.

* darraghrooney@gmail.com
† abloch@umich.edu
‡ rangan@uwindsor.ca

In section II of this paper, we decompose the Lindblad master equation into its inter- and intra-orbit components, and interpret the resulting ODE as a control equation. In section III, we derive an adjustment equation that maintains critical points as purity varies. We consider the special cases where the adjustment equation fails. In section IV, we derive the adjustment that maintains zeros. In section V we show several examples that illustrate the effect of the Lindblad super-operator on the Bloch ball.

II. PRELIMINARIES

An open quantum system is described by a density operator ρ, which is a trace-one positive semi-definite operator on the Hilbert space $\mathcal{H}$. If the dissipation is Markovian and time-independent, the density operator obeys the Lindblad equation [10]:

$$\frac{d}{dt}\rho(t) = [-iH(t), \rho(t)] + \mathcal{L}_D(\rho(t)) \tag{1}$$

$$\mathcal{L}_D(\rho) := \sum_{m=1}^{N} L_m \rho L_m^\dagger - \frac{1}{2}\{L_m^\dagger L_m, \rho\}, \tag{2}$$

where the braces indicate an anti-commutator, $H(t)$ is the (Hermitian) Hamiltonian, and $\{L_m\}$ are the so-called Lindblad operators.

For $n = 2$, the density operator can be identified with the Bloch vector $\vec{n} \in \mathbb{R}^3$, $|\vec{n}| \leq 1$. The identification is:

$$\rho = \frac{1}{2}\left(I_2 + \sum_{j=x,y,z} n_j \sigma_j\right), \tag{3}$$

where $\{\sigma_j\}$ are the Pauli matrices. The Lindblad equation translates to the following ODE (see Appendix A for a derivation):

$$\frac{d\vec{n}}{dt} = \vec{b} + \vec{h} \times \vec{n} + (A - \mathrm{tr}(A))\vec{n}. \tag{4}$$

Here we write $\vec{h}$ and $\vec{l}_m$ to represent the traceless parts of the operators H and L_m, expressed in the basis of the Pauli matrices, so that $H = h_0 I + \sum_{j=1}^{3} h_j \sigma_j$. The system parameters are defined:

$$A := \frac{1}{2}\sum_m \vec{l}_m \bar{\vec{l}}_m^T + \bar{\vec{l}}_m \vec{l}_m^T \tag{5}$$

$$\vec{b} := i \sum_m \vec{l}_m \times \bar{\vec{l}}_m, \tag{6}$$

where the bar represents complex conjugate and T matrix transpose. A is a positive semi-definite matrix, so its eigenvalues a_j must be non-negative. Additionally, the vector $\vec{b}$ obeys the inequality (see Appendix B):

$$\vec{b}^T A \vec{b} \leq 4 \det(A). \tag{7}$$

The objects A and $\vec{b}$ can be interpreted as damping parameters (see appendix C). Since A is symmetric, it has a natural coordinate frame, and the system is damped parallel to these coordinate axes. The eigenvalues of A specify damping rates $r_1 = a_2 + a_3$ etc. If $\vec{b}$ is zero, the system relaxes to $\vec{n} = 0$; otherwise we say the damping is biased, and it relaxes to a point with coordinates $\frac{b_j}{r_j}$ in the coordinate system of A. We refer to $\vec{b}$ as the damping-bias vector.

We would like to decompose the ODE into its radial and transverse components. Each concentric sphere in the Bloch ball corresponds to a particular unitary orbit of density matrices (including the center). The eigenvalues $\lambda_1 \geq \lambda_2$ of ρ can be calculated from the radius $r := |\vec{n}|$ of each sphere: $\lambda_{1,2} := \frac{\mathrm{tr}(\rho)}{2} \pm \sqrt{\frac{\mathrm{tr}(\rho)^2}{4} - \det(\rho)} = \frac{1 \pm r}{2}$, and therefore $r = \lambda_1 - \lambda_2$. Since each unitary orbit is uniquely described by an eigenvalue spectrum of ρ, there is a one-to-one correspondence between the unitary orbits and the radial component $r \in [0, 1]$.

The transverse component, on the other hand, exists either on a concentric sphere if $r > 0$, or a singleton-set if $r = 0$. In fact, each orbit is a (complex) flag manifold [22]. A *flag* is a nesting of subspaces $\emptyset \subset V_1 \subset V_1 \oplus V_2 \subset \cdots \subset V_1 \oplus V_2 \oplus \cdots \oplus V_n$. In our case, these subspaces are the eigenspaces of ρ. When $r = 0$, the nesting is trivial: $\emptyset \subset \mathcal{H}$. When $r > 0$, we set V_1 and V_2 to be the eigenspaces corresponding to λ_1 and λ_2, and therefore each flag is $\emptyset \subset V_1 \subset \mathcal{H}$. Choosing a flag is tantamount to choosing the leading eigenvector of ρ. In the Bloch ball picture, this flag can be described by a unit vector $\hat{n}$, where $\vec{n} = r\hat{n}$. For the rest of the paper, we will use the term *flag* interchangeably with $\hat{n}$ when $r > 0$. Because our approach is based on manipulating $\hat{n}$, we call it *flag-based control*. In using the word "flag" as opposed to "unit vector", we both include the $r = 0$ case, as well as prepare for generalizing to higher dimensions where the Bloch ball picture cannot be used. The authors are preparing a paper thats considers systems of arbitrary finite dimension [26].

To decouple the ODE, we use the product rule: $\frac{d\vec{n}}{dt} = \frac{dr}{dt}\hat{n} + r\frac{d\hat{n}}{dt}$, which yields $\frac{dr}{dt} = \hat{n} \cdot \frac{d\vec{n}}{dt}$, as well as $\frac{d\hat{n}}{dt} = -\frac{1}{r}\hat{n} \times (\hat{n} \times \frac{d\vec{n}}{dt})$. Then we have:

$$\frac{dr}{dt} = \vec{b} \cdot \hat{n} + r\,(\hat{n} \cdot A\hat{n} - \mathrm{tr}(A)) =: f(\hat{n}, r) \tag{8}$$

$$\frac{d\hat{n}}{dt} = -\frac{1}{r}\vec{b}_\perp + \vec{h} \times \hat{n} - (A\hat{n})_\perp, \tag{9}$$

where the $\perp$ subscript indicates the component perpendicular to $\hat{n}$.

The behavior at $r = 0$ demands attention. Clearly, $\frac{d\hat{n}}{dt}$ can be quite large for small r, but for trajectories that pass through $\vec{n} = 0$, it is well behaved. At this point, $\frac{d\vec{n}}{dt} = \vec{b}$, which means that shortly before or after, we have $\vec{n} = \vec{b}\,\delta t$. It follows that $r = |\vec{b}\,\delta t|$ and $\hat{n} = \mathrm{sgn}(\delta t)\hat{b}$. The

ODE's then give:

$$\frac{dr}{dt} = \mathrm{sgn}(\delta t)|\vec{b}| + O(\delta t) \tag{10}$$

$$\frac{d\hat{n}}{dt} = \mathrm{sgn}(\delta t)\left(\vec{h}\times\hat{b} - (A\hat{b})_\perp\right), \tag{11}$$

which are clearly bounded.

III. MAXIMIZING AND MINIMIZING THREADS

In a control-theoretic context, we are typically able to choose the Hamiltonian $H(t)$ to some degree. The Hamiltonian appears only in the transverse equation (9), while the radial component (8) has no explicit Hamiltonian dependence. We are interested in the question of how to steer the transverse component in order to influence the radial. We will presume that we have fast and complete controllability, *i.e.*, in the absence of Lindblad dissipation, we are able to steer between any two points on an orbit in arbitrarily short time (or at least in a time-scale much shorter than that associated with the Lindblad operators). This means we can consider $\hat{n}$ to be an effective control variable: we can search for desirable $\hat{n}(t)$ and then re-construct $H(t)$ afterwards.

Given this context, we are interested in optimizing the function $f_r(\hat{n}) := f(\hat{n}, r)$ for a given r. That is, we would like to find the point on an orbit that optimizes the inter-orbit speed. This can be done using the method of Lagrange multipliers for $|\hat{n}| = 1$ [27][23], which gives, for the multiplier ν, the conditions

$$\vec{b} + 2rA\hat{n} = 2\nu\hat{n}, \tag{12}$$

and

$$|\hat{n}| = 1. \tag{13}$$

This leads in the general case to the degree-six polynomial in ν:

$$\sum_{j=1}^{3} b_j^2(\nu - ra_{[j+1]})^2(\nu - ra_{[j+2]})^2 - \prod_{j=1}^{3}(\nu - ra_j)^2 = 0, \tag{14}$$

where the square brackets indicate modular addition, so that the indices cycle through 1, 2 and 3.

This approach will not scale up nicely to higher dimensions, since it will involve solving systems of high-degree polynomials. Instead we try a different tack with better scalability. It is easy to analyze $f_0(\hat{n}) = \vec{b}\cdot\hat{n}$. It is clear that f_0 is maximized at $\hat{n}_+ := \hat{b}$, minimized at $\hat{n}_- := -\hat{b}$ and zero for any vector perpendicular to $\vec{b}$. Now if we continuously increase r from zero, we investigate whether there are differentiable functions $\hat{n}_\pm(r)$, with adjustment $\vec{m}_\pm(r) := \frac{d}{dr}\hat{n}_\pm(r)$ such that $\hat{n}_\pm(r)$ are local optima for the functions $f_r(\hat{n})$ for every r. If such functions exist, we call the corresponding differentiable curves $\vec{n}_\pm(r) := r\hat{n}_\pm(r)$ maximizing and minimizing *threads*.

We know that $\hat{n}$ lives on the sphere S^2, and a tangent space to S^2 can be identified with the two-dimensional vector space of vectors perpendicular to $\hat{n}$. The derivative of f_r at a point $\hat{n}$ with respect to a variation $\vec{\epsilon}$ can be written as

$$df_r(\hat{n})\cdot\vec{\epsilon} = \vec{b}^T\vec{\epsilon} + 2r\hat{n}^T A\vec{\epsilon} \tag{15}$$

$$= (\vec{b} + 2rA\hat{n})^T\vec{\epsilon}. \tag{16}$$

Note that $df_0(\pm\hat{b})\cdot\vec{\epsilon} = \vec{b}^T\vec{\epsilon} = 0$, since $\hat{n}$ and $\vec{\epsilon}$ must be orthogonal. It follows that $\hat{n} = \pm\hat{b}$ are critical points of f_0, and in fact they are the only two critical points.

Our objective is to vary $\hat{n}$ with r so that it remains a critical point of f_r. To this end, we differentiate the equation $df_r(\hat{n})\cdot\vec{\epsilon} = 0$ with respect to r. We must be careful however since the tangent spaces at each $\hat{n}$ are different. We must also vary $\vec{\epsilon}$ so that it remains perpendicular to $\hat{n}$. Let $\vec{m} := \frac{d\hat{n}}{dr}$ and $\vec{\mu} := \frac{d\vec{\epsilon}}{dr}$. Since $\hat{n}(r)\cdot\vec{\epsilon}(r) = 0$, $\vec{\mu}$ must always satisfy $\hat{n}\cdot\vec{\mu} = -\vec{m}\cdot\vec{\epsilon}$ (from the product rule). We now have:

$$\frac{d}{dr}\left(df_r(\hat{n})\cdot\vec{\epsilon}\right) = \frac{\partial}{\partial r}\left(df_r(\hat{n})\cdot\vec{\epsilon}\right) + (2rA\vec{m})^T\vec{\epsilon} + (\vec{b} + 2rA\hat{n})^T\vec{\mu} \tag{17}$$

$$= (2A\hat{n} + 2rA\vec{m})^T\vec{\epsilon} + (\vec{b} + 2rA\hat{n})^T\vec{\mu}. \tag{18}$$

If $\hat{n}$ is a critical point of f_r, the vector $\vec{b} + 2rA\hat{n}$ is parallel to $\hat{n}$. Let the norm of this vector be C. We now have:

$$\frac{d}{dr}\left(df_r(\hat{n})\cdot\vec{\epsilon}\right) = (2A\hat{n} + 2rA\vec{m})^T\vec{\epsilon} + C\hat{n}^T\vec{\mu} \tag{19}$$

$$= (2A\hat{n} + 2rA\vec{m})^T\vec{\epsilon} - C\vec{m}^T\vec{\epsilon} \tag{20}$$

$$= (2A\hat{n} + \Lambda\vec{m})^T\vec{\epsilon}, \tag{21}$$

where $\Lambda := 2rA - C$. If we want this expression to vanish for arbitrary $\vec{\epsilon}$ perpendicular to $\hat{n}$, we need to have, for some real k:

$$2A\hat{n} + \Lambda\vec{m} = k\hat{n} \tag{22}$$

$$\vec{m} = \Lambda^{-1}(k - 2A)\hat{n}, \tag{23}$$

where k can be found by projecting both sides on to $\hat{n}$:

$$k = 2\frac{\hat{n}^T\Lambda^{-1}A\hat{n}}{\hat{n}^T\Lambda^{-1}\hat{n}}. \tag{24}$$

We can now state the following proposition:

Proposition III.1. *Consider a point $(r_0, \hat{n}_0) \in [0,1]\times S^2$ that is critical, in the sense that $df_{r_0}(\hat{n}_0)\cdot\vec{\epsilon}$ vanishes for any $\vec{\epsilon}$ perpendicular to $\hat{n}_0$. Define:*

$$k(r,\hat{n}) := 2\frac{\hat{n}^T\Lambda(r,\hat{n})^{-1}A\hat{n}}{\hat{n}^T\Lambda(r,\hat{n})^{-1}\hat{n}} \tag{25}$$

$$\Lambda(r,\hat{n}) := 2rA - C(r,\hat{n}) \tag{26}$$

$$C(r,\hat{n}) := \hat{n}^T(\vec{b} + 2rA\hat{n}). \tag{27}$$

If there is an open set $\Omega \subseteq [0,1] \times S^2$ containing $(r_0, \hat{n}_0)$, over which (1) $\Lambda(r,\hat{n})$ is invertible, and (2) $\hat{n}^T \Lambda(r,\hat{n})^{-1}\hat{n} \neq 0$, then the ODE

$$\frac{d\hat{n}}{dr} = \Lambda(r,\hat{n})^{-1}(k(r,\hat{n}) - 2A)\hat{n}, \tag{28}$$

has a unique solution $\hat{n}(r)$ on some interval $[r_0, r_f)$, and every point on this solution satisfies $df_r(\hat{n}(r)) \cdot \vec{\epsilon} = 0$, $\forall \epsilon$ perpendicular to $\hat{n}(r)$.

If the conditions on $\Lambda(r,\hat{n})$ hold for all points on $[0,1] \times S^2$, there exist two threads, $\hat{n}_\pm(r)$, that satisfy the ODE and have initial conditions $(r_0, \hat{n}_{0\pm}) = (0, \pm\hat{b})$.

Proof. The local existence and uniqueness result is an application of standard theory of ODE's on manifolds [28]. Local existence requires differentiability of the RHS, which clearly holds given the two conditions. The vanishing of the derivative has already been shown. The global existence result holds because $[0,1] \times S^2$ is compact. □

Both of the conditions on $\Lambda(r,\hat{n})$ sometimes fail, which we shall discuss in section V. The first is always tractable, while analysis of the second requires the solution of a polynomial. Apart from these special cases however, we now have two functions $\hat{n}_\pm(r)$ with $\hat{n}_\pm(0) = \pm\hat{b}$ and $\frac{d}{dr}\hat{n}_\pm = \vec{m}(\hat{n}_\pm)$ that optimize (at least locally) $f_r(\hat{n})$ for each r.

IV. TRAJECTORY PLANNING

We now have an adjustment $\vec{m} = \frac{d\hat{n}}{dr}$ that ensures a trajectory remains on a critical point as it moves inward to or outward from the completely mixed orbit. Our control variable however is the Hamiltonian, so to plan a trajectory (for example, to move from the completely mixed state $r = 0$ outwards), we must know how to recover an appropriate Hamiltonian from a given adjustment.

We know previously that $\frac{d\hat{n}}{dt} = -\frac{1}{r}\vec{b}_\perp + \vec{h} \times \hat{n} - (A\hat{n})_\perp$. We also know $\frac{d\hat{n}}{dr} = \vec{m}$. If we write $\frac{d\hat{n}}{dt} f(r,\hat{n}) = \frac{d\hat{n}}{dt}$, we get

$$\vec{m}(r,\hat{n}) f(r,\hat{n}) = \vec{h} \times \hat{n} - \frac{1}{r}\vec{b}_\perp - (A\hat{n})_\perp \tag{29}$$

$$\vec{h} = \hat{n} \times \left(\vec{m}(r,\hat{n}) f(r,\hat{n}) + \frac{1}{r}\vec{b}_\perp + (A\hat{n})_\perp \right). \tag{30}$$

Note that the term $\frac{1}{r}\vec{b}_\perp$ is well-behaved since $\vec{b} \times \hat{n}$ is zero at $r = 0$ and $O(r)$ in the vicinity. Also note that an arbitrary component parallel to $\hat{n}$ can be added to $\vec{h}$. In short, to attain a desired trajectory $\hat{n}(r)$ using its associated adjustment $\vec{m}(r,\hat{n})$, one should apply a radially varying Hamiltonian in the form

$$\vec{h}(r) = c(r)\hat{n}(r) + \hat{n}(r) \times \left(\vec{m}(r,\hat{n}(r)) + \frac{1}{r}\vec{b} + A\hat{n}(r) \right), \tag{31}$$

where $c(r)$ is arbitrary.

One might think the piece including $\vec{m}$ may blow up if Λ becomes non-invertible, but we will see that this is not the case. There are cases where $\vec{m}$ does blow up, but this does not occur on the main threads $\hat{n}_\pm(r)$ that arise at $r = 0$. Instead, this occurs when alternate threads arise at some $r > 0$. We discuss these possibilities in the next section.

V. SPECIAL CASES

We now consider the instances in which the adjustment may not be well-defined, either due to (1) Λ losing invertibility, or (2) the denominator in the definition of k vanishing. The matrix Λ loses invertibility if and only if the constant C equals one of the eigenvalues a_j of $2rA$. But at any critical point, we have:

$$\vec{b} + 2rA\hat{n} = C\hat{n} \tag{32}$$

$$\vec{b} = -\Lambda\hat{n}. \tag{33}$$

In other words, degeneracy of Λ implies that $\vec{b}$ must be in the image of Λ, which does not have full dimension. We separate the cases based on the multiplicity of the eigenvalue of $2rA$ in question.

(1a) C is a triple eigenvalue of $2rA$.
This case is largely trivial. If A is a multiple of the identity aI_2, where a is the only eigenvalue of A, and $C = 2ra$, then $\Lambda = 0$, and therefore $\vec{b} = 0$. We have then:

$$f_r(\hat{n}) = -2ar \tag{34}$$

$$df_r(\hat{n}) \cdot \vec{\epsilon} = 2ra\hat{n}^T\vec{\epsilon} = 0. \tag{35}$$

Therefore all possible $\hat{n}$ are critical points of f_r due to the rotational symmetry. No optimization is needed since f_r is a constant function.

(1b) C is a double eigenvalue of $2rA$.
In this case, we find a plane of critical points that intersect one of the main threads $\hat{n}_\pm(r)$. Additionally, this case covers the well-studied phase- and amplitude-damping channels.

Let $\{e_j\}$, $j = 1,2,3$, be an eigenbasis of A, where the eigenvalues a_1 and a_2 are equal, and $a_3 \neq a_1$. It follows that for $C = 2ra_1$, we need $\hat{b} = e_3$. We know critical points satisfy $\vec{b} + 2rA\hat{n} = C\hat{n}$, which gives:

$$2ra_1\hat{n}_j = C\hat{n}_j, \;\; j = 1,2 \tag{36}$$

$$b_3 + 2ra_3\hat{n}_3 = C\hat{n}_3. \tag{37}$$

There are two solutions. If $\hat{n}_1 = \hat{n}_2 = 0$, then $\hat{n}_3 = \pm 1$. This solution corresponds to the main threads $\hat{n}_\pm(r) = \pm\mathrm{sgn}(b_3)$. In this case, no adjustment is needed, since eq. (22) is satisfied for $\vec{m} = 0$. As it happens, $C = \pm b_3 + 2ra_3$, which means that $\Lambda_\pm = \mp b_3 I + 2r(a_1 - a_3)\cdot$

$\mathrm{diag}(1,1,0)$. Invertibility is lost at $r = \frac{|b_3|}{2|a_1-a_3|}$, but yet the adjustment solution $\vec{m}=0$ is still valid there.

An alternate solution exists. If $C = 2a_1 r$, then $\hat{n}_1$ and $\hat{n}_2$ are free. In this case, $n_3 = r\hat{n}_3 = \frac{b_3}{2(a_1-a_3)}$. So there is a plane of critical points, that happens to orthogonally intersect one of the main threads at exactly the point where the corresponding Λ loses invertibility. On this critical plane, Λ is everywhere non-invertible: it is equal to $\mathrm{diag}(0,0,2r(a_3-a_1))$. Yet any $\vec{m}$ with $m_3 = \frac{b_3}{2r^2(a_3-a_1)}$ satisfies eq. (22). This solution allows a valid $\vec{m}$, unless $\hat{n}$ approaches the intersection point with the main thread. Since $\vec{m}$ and $\hat{n}$ must be perpendicular, some combination of the components m_1 and m_2 must grow unbounded, and at the intersection point itself, there is no solution since perpendicularity forces $m_3 = 0$. This also implies that one cannot switch from the main thread to the alternate plane.

We can apply this to a combination of phase- and amplitude-damping channels [25]. A phase-damping channel uses a Lindblad operator in the form $L_z := \sqrt{\gamma_z}\sigma_z$, while the amplitude-damping channel uses Lindblad operators in the form $L_\pm := \sqrt{\gamma_\pm}\sigma_\pm$, where $\sigma_\pm = \frac{\sigma_x \mp i\sigma_y}{2}$. In this case, we get the following parameters: $a_1 = \gamma_z$, $a_2 = a_3 = \frac{\gamma_+ + \gamma_-}{4}$ and $\vec{b} = \langle \frac{\gamma_+ - \gamma_-}{2}, 0, 0\rangle$. Since $b_2 = b_3 = 0$ and $a_2 = a_3$, we have a plane of critical points at $e_1 \cdot \vec{n} = \frac{\gamma_+ - \gamma_-}{4\gamma_z - \gamma_+ - \gamma_-}$.

(1c) C is a single eigenvalue of $2rA$.
This case is similar to the preceding, except the plane of critical points is now a line of critical points. Let $C = 2ra_1$ and $a_1 \neq a_2, a_3$, we still have $b_1 = 0$. We get:

$$2a_1 r\hat{n}_1 = C\hat{n}_1 \tag{38}$$

$$b_j + 2a_j r\hat{n}_j = C\hat{n}_j, \quad j = 2,3 \tag{39}$$

As before, choosing $\hat{n}_1 = 0$ allows us to recover the main threads $\hat{n}_\pm(r)$. C will equal the offending value $2ra_1$ at $r = \sqrt{\frac{b_2^2}{4(a_1-a_2)^2} + \frac{b_3^2}{4(a_1-a_3)^2}}$. The fact that Λ loses invertibility here does not affect the adjustment, because the direction of degeneracy happens to be orthogonal to $\hat{n}$: that is, Λ is degenerate in the e_1-direction. Therefore the adjustment can still be found.

An alternate thread can be found by setting $C = 2ra_1$ and letting $\hat{n}_1$ run free. In this case, we find that $n_j = r\hat{n}_j = \frac{b_j}{2(a_1-a_j)}$, so this thread is orthogonal to the $\hat{n}_1 = 0$ plane. While Λ is non-invertible on this thread, we can find a solution to eq. (22): m_1 can be free, while $m_2 = -n_2$ and $m_3 = -n_3$. To satisfy perpendicularity, however, we require $m_1 = \frac{n_2^2+n_3^2}{n_1}$. This clearly blows up as the thread crosses the $n_1 = 0$ plane.

Note the alternate thread may or may not intersect the main threads, but from our simulations, we observe that intersections only seem to occur when $a_2 = a_3$.

(2) k is not well-defined.
The above cases are simpler than a generic system, since a component of $\vec{b}$ vanishes in the natural co-ordinates of A, which reduces the degree of equation (14) from six to four (or two). However, it may still happen that Λ is invertible, yet $\hat{n}^T\Lambda^{-1}\hat{n} = 0$. In this case, the algebra required to find such a location still leads to a degree-six polynomial. We essentially have five unknowns: r, C and the three components of $\hat{n}$. These obey five equations:

$$b_j + 2ra_j\hat{n}_j = C\hat{n}_j \tag{40}$$

$$|\hat{n}| = 1 \tag{41}$$

$$\sum_j \frac{\hat{n}_j^2}{2ra_j - C} = 0, \tag{42}$$

where the final equation is the failure of condition (2). We can eliminate the variable r and the second equation by working with the components of $\vec{n}$ instead of $\hat{n}$. Furthermore, working with $\mu = \frac{C}{2r}$ yields $n_j = \frac{b_j}{2(a_j-\mu)}$. Substitution into the third equation gives $\sum_j \frac{b_j^2}{8(a_j-\mu)^3} = 0$. This yield the sixth-degree polynomial equation:

$$b_1^2(a_2-\mu)^3(a_3-\mu)^3 + b_2^2(a_3-\mu)^3(a_1-\mu)^3 + b_3^2(a_1-\mu)^3(a_2-\mu)^3 = 0. \tag{43}$$

One can find solutions numerically for μ and the corresponding $\vec{n}$ follows easily. Such a solution corresponds to an alternate thread of critical points: when such a thread becomes tangent to a concentric sphere in the Bloch ball, the adjustment $\vec{m}$ becomes infinite, which is why the adjustment expression fails. It is possible to plot such an alternate thread by locating an initial point away from where the adjustment fails, and then using the adjustment in either direction. To locate such a point, one needs to solve the degree-six polynomial (14). We will not do this in our examples, as it contradicts the spirit of this paper. In higher dimensions, the algebra would not be tractable, therefore we must make peace with the fact that the adjustment works only to find critical points locally.

VI. SEPARATION OF THE BLOCH BALL

Besides finding the optimal points of f_r, it is also an interesting question to locate the zeros of f_r. It turns out that for $\vec{b} \neq 0$, there is a "chimney" region in the Bloch ball, inside of which the purity "rises". That is, $f(\hat{n}, r) > 0$, and outside of which $f(\hat{n}, r) < 0$. If we want r to increase, we must steer inside of this region. We can locate the "wall" of this chimney by using another adjustment expression. We know that at $r = 0$, we have $f_0(\hat{n}) = 0$ for $\hat{n} \cdot \vec{b} = 0$, which has a S^1-homeomorphic set of solutions, say $\hat{c}_\theta$, with $\theta \in [0, 2\pi)$ being an angle parameter. We want to take such a solution, use it as an inital condition, and find an adjustment to ensure $f_r(\hat{n}) = 0$ as r increases. To do this, we differentiate f_r

with respect to r, with $\vec{m} = \frac{d\hat{n}}{dr}$:

$$\frac{d}{dr}\left(f_r(\hat{n})\right) = \frac{\partial}{\partial r} f_r(\hat{n}) + \nabla_{\hat{n}} f_r(\hat{n}) \cdot \vec{m} \tag{44}$$

$$= \hat{n}^T A \hat{n} - \mathrm{tr}(A) + (\vec{b} + 2rA\hat{n})^T \vec{m} \tag{45}$$

$$(\vec{b} + 2rA\hat{n})^T \vec{m} = \mathrm{tr}(A) - \hat{n}^T A \hat{n}. \tag{46}$$

To satisfy this equation, as well as $\vec{m} \cdot \hat{n} = 0$, define $\vec{v} = \vec{b} + 2rA\hat{n}$. A possible solution is:

$$\vec{m} = \frac{\mathrm{tr}(A) - \hat{n}^T A \hat{n}}{|\vec{v}|^2 - (\hat{n} \cdot \vec{v})^2} \left(\vec{v} - (\hat{n} \cdot \vec{v})\hat{n}\right). \tag{47}$$

This solution is not unique: for a given r, there is a continuum of zeros of f_r, at least until the chimney terminates. If we kept r fixed, and moved along this continuum with $\hat{n} = \hat{n}(t)$, an adjustment $\frac{d\hat{n}}{dt} \propto \hat{n} \times \vec{v}$ would ensure $f_r(\hat{n}(t)) = 0$. For our adjustment, we will thus keep the component parallel to $\hat{n} \times \vec{v}$ zero, so that we capture only the necessary motion of $\hat{n}$.

Of course, the adjustment will terminate for some $r \leq 1$, since f_r cannot be positive at that radius. The terminating condition is $\hat{n} \cdot \vec{v} = |\vec{v}|$, which matches the critical point condition. At such a point, the adjustment becomes infinite. Thus the point on the chimney furthest from the origin (which we call the *apogee*) is a critical point, either on the maximizing thread $\hat{n}_\pm$, or possibly on one of the alternate threads. In the following section, we will show examples of both possibilities.

Finally, it should be noted that the chimney does have an analytic solution. If one uses $r f_r(\hat{n}) = 0$ and substitutes $r^2 = \vec{n}^2$, we obtain an elllipsoid in the co-ordinates of $\vec{n}$:

$$\sum_j \tilde{a}_j \left(n_j - \frac{b_j}{2\tilde{a}_j}\right)^2 = \sum_j \frac{b_j^2}{4\tilde{a}_j}, \tag{48}$$

where $\tilde{a}_1 := a_2 + a_3$ and so forth. In general however, the ellipsoid center and axes are not aligned with the axes of A, other than intersecting the center of the Bloch ball. So the intersection of the ellipsoid with concentric spheres, which is what we are interested in, will not have a clean analytic expression. In fact the intersection may not even be connected: this is what happens when there is more than one apogee.

VII. EXAMPLES

The adjustment (23) and (47) can be used to form ODE's $\frac{d}{dr}\hat{n} = \vec{m}(r, \hat{n})$ with initial conditions $\hat{n}_\pm(0) = \pm\hat{b}$ or $\hat{n}_\theta(0) = \hat{c}_\theta$ that can be solved numerically. The chimney can be plotted by discretizing the circle of initial points and calculating threads on the chimney. We have implemented this using a Runge-Kutta method for Lie groups [29] which ensures $\hat{n}$ remains normalized. The results are consistent with the preceding analysis. Fig. 1 shows a typical example. The interval $r \in [0, 1]$ has been discretized into intervals of length $\frac{1}{1000}$. The maximizing thread curls towards the upper right, and the minimizing thread to the lower left. We have estimated the error by calculating the component of $\vec{b} + 2rA\hat{n}$ perpendicular to $\hat{n}$, and we can report that this error does not exceed 3×10^{-10} for either thread in this example. Typically a discretization of $\delta r = \frac{1}{1000}$ is sufficient to achieve precision of such order.

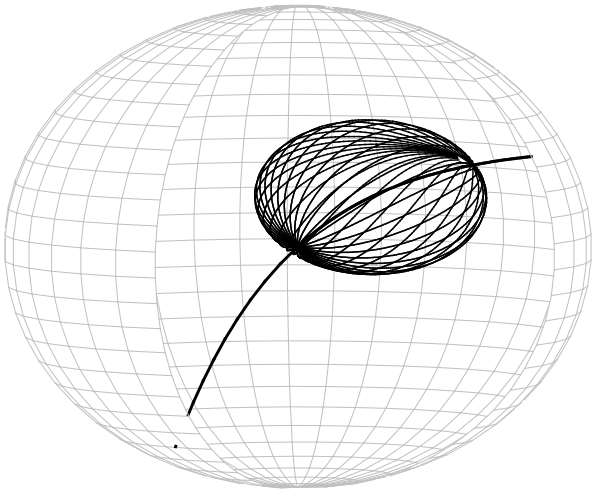

FIG. 1. Optimizing threads and chimney for $A = \mathrm{diag}(100, 57, 39)$ and $b = \langle 29, 67, 61\rangle$. Inside the chimney, the dynamics drives the Bloch vector outwards, whereas Bloch vectors outside have negative radial velocity. The thread represents points that have optimal radial velocity. The piece from the center to the lower left has minimal velocity, while the piece in the upper right has maximal velocity.

The chimney is also plotted by discretizing the circle of initial points into thirty-six. It is important to note that the algorithm is not capable of finding the apogee of the chimney, since the ODE blows up there. One must stop the algorithm when the error exceeds a certain threshold. For the chimney we estimate the error by calculating $f_r(\hat{n}_\theta(r), r)$, and we can report for this example the error does not exceed 2.5×10^{-6}. The threshold we used was 1×10^{-3}. For this example, the chimney threads finish near the maximizing thread, so we can infer that their termination point lies on this thread. The termination point can be calculated by finding the zero of $f(\hat{n}_+(r), r)$. There are no alternate threads for this example.

In fig. 2, we have an example with an alternate thread. Since $b_1 = 0$ and $a_2 = a_3$, we know there will be a line of critical points that intersects the maximizing thread. The alternate thread of critical points is horizontal in the plot, with thinner line-width. When we plot the chimney we can see that all but two of the thirty-six chimney threads terminate on the alternate thread, rather than the maximizing thread. Below the Bloch ball we also plot $f(\hat{n}_\pm(r), r)$ with thick line-width and $f(\hat{n}_a(r), r)$ with thin line-width, where $\hat{n}_a$ is the alternate thread. We can see that the maximizing thread only gives a local maximum for radii at which the alternate thread exists,

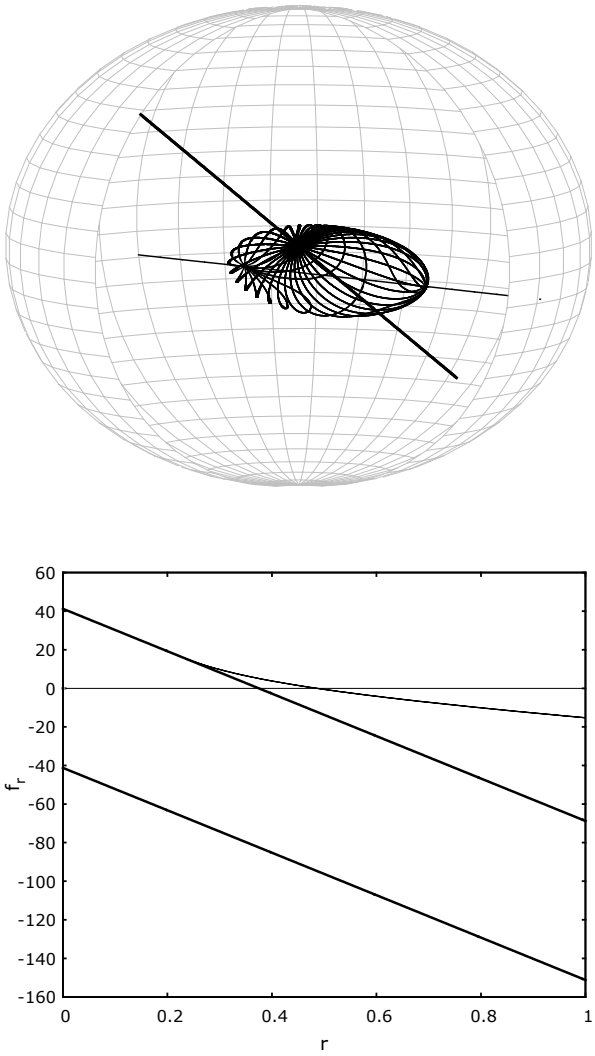

FIG. 2. (Top) The main threads are represented by the thick line, while the transverse line represents an alternate thread. $A = \mathrm{diag}(100, 10, 10)$ and $b = \langle 0, 32, -26\rangle$. (Bottom) $f(\hat{n}_\pm, r)$ and $f(\hat{n}_a, r)$ for the same system. Thick lines represent radial velocity of the main threads, while the thinner line represents the radial velocity of the alternate thread. Clearly, the alternate thread is the global maximum on its domain.

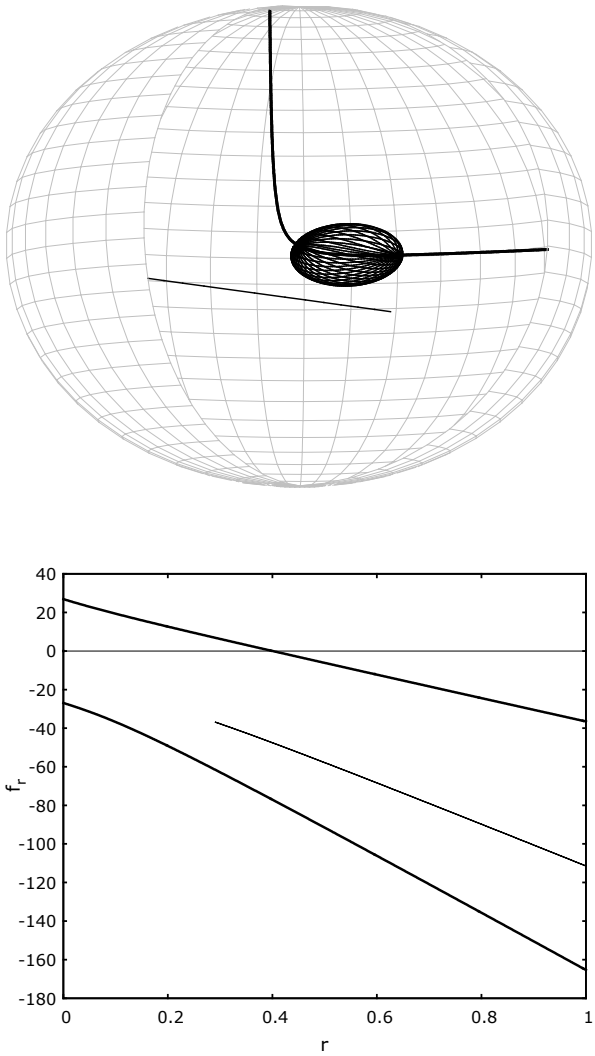

FIG. 3. (Top) The main threads that pass through the chimney are shown in bold, while an alternate thread also exists. There is no intersection, as $a_2 \neq a_3$. $A = \mathrm{diag}(100, 50, 10)$ and $b = \langle 23, 0, -14\rangle$. (Bottom) $f(\hat{n}_\pm, r)$ and $f(\hat{n}_a, r)$ for the same system. The thinner line represents the radial velocity of the alternate thread. Clearly the alternate thread is not a global optimum.

and the alternate thread provides the global maximum.

In fig. 3, we have another example with an alternate thread. This time $b_2 = 0$ and $a_1 \neq a_3$, and and we see the line of critical points does not intersect the optimizing threads. When we plot $f(\hat{n}_\pm(r), r)$ and $f(\hat{n}_a(r), r)$, we can see the alternate thread does not provide a global optimum, and the optimizing threads provide global optima for all r.

In fig. 4, we have an example where $b_j \neq 0$, and yet there is still an (unshown) alternate thread. While nineteen of the thirty-six chimney threads terminate on the maximizing thread, the remaining seventeen clearly terminate elsewhere, and so the chimney has a second apogee. In fact, there is an alternate thread that begins inside the chimney and exits at this hole (there is another exit point that does not serve as a termination point, because it is a saddle point). In keeping with the spirit of this paper, we have not attempted to plot this alternate thread or determine whether it provides a global optimum. We can report that the termination point on the maximizing thread is at a larger radius ($r \cong 0.748$) than the alternate termination point ($r \cong 0.649$).

We have however decided to estimate how often a system has an alternate thread. We have simulated 100,000 random systems in the following way: the largest eigenvalue of A was fixed to be $a_1 = 100$. The remaining two were chosen to be uniform on the interval $[0, 100]$. To randomize $\vec{b}$ we know that, due to the positive-definiteness of

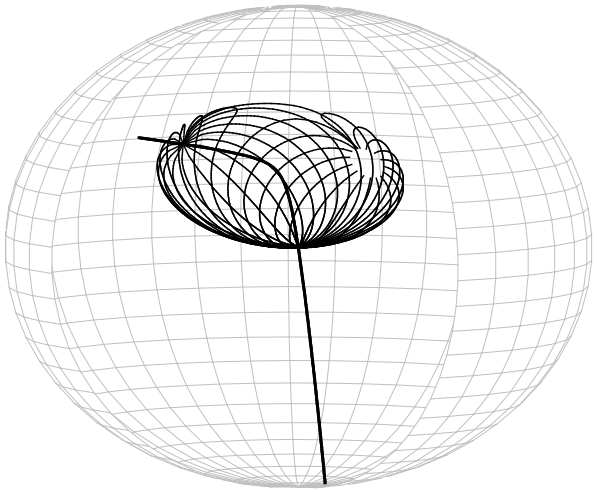

FIG. 4. A system with main threads, and and unshown alternate thread. The main threads optimize radial velocity locally. However, the fact that chimney lines approach a point that is clearly not on the main threads indicates there is an alternate thread that also locally maximizes radial velocity. $A = \mathrm{diag}(100, 16, 11)$ and $b = \langle -3, -8, 68\rangle$.

the GKS matrix [11], it obeys the inequality (B3). Thus the vector $\vec{b}^* = \langle \frac{b_1}{2\sqrt{a_2 a_3}}, \frac{b_2}{2\sqrt{a_1 a_3}}, \frac{b_3}{2\sqrt{a_1 a_2}}\rangle$ must lie in a ball of radius one. We impose a uniform distribution on this ball, choose a $\vec{b}^*$ and calculate $\vec{b}$. With this randomization, we conducted 100,000 simulations that yielded 59,830 systems without an alternate thread, 30,811 with one alternate thread and 9,359 with two.

VIII. CONCLUSIONS AND FUTURE WORK

We have demonstrated that it is possible to derive an adjustment equation that maintains critical points and zeros as one transitions between quantum orbits. The behavior at the completely mixed state is easy to analyze: both the critical points and the zeros of the function $f(r, \hat{n}) = \frac{dr}{dt}$ are trivial to compute at that orbit. As one increases r, these zeros and critical points can be preserved. The critical points form two threads: one of which maximizes $\frac{dr}{dt}$ locally, the other minimizes. If one has fast controllability and one wants to optimize the speed at which the state moves between orbits, the system can be steered to either of these threads, depending on the desired direction. The adjustment expression also yields an expression for a Hamiltonian that keeps the system on the thread.

It is important to note that this mechanism only ensures that the optima are local. There are systems where other optima emerge as one moves away from the completely mixed state. Sometimes such an alternate optimum is also the global optimum, sometimes not.

We have used a general framework that includes all possible Lindblad processes. This framework describes Lindblad dissipation in terms of three phase-damping processes and a damping-bias vector. Our approach is useful for biased damping: if $\vec{b} = 0$ and all damping rates are non-zero, the system relaxes inextricably to the completely mixed state. In the presence of biased damping however, the Hamiltonian can be used to guide the system to its optimal relaxation point, at the apogee of the chimney.

A paper by us considering flag-based control in arbitrary finite dimensions is in press [26]. In this paper, we formally consider the decomposition of ρ into its flag and eigenvalue spectrum for $2 \leq n < \infty$. The intention of the follow-up paper is only a first attempt at flag-based control, and as such, more work has gone into treating the decomposition of ρ, rather than obtaining sophisticated control results. In particular, the control results obtained therein are for a discrete control set of flags. This is in contrast to this paper, where we specifically examine continuous adjustment of the flag.

Nevertheless, we believe that the continuous adjustment process treated in this paper can be generalized to higher dimensions. Because the Lindblad term $\mathcal{L}_D(\rho)$ in dimension n reduces to $\frac{1}{n}\sum_m [L_m, L_m^\dagger]$ at the completely mixed state, it can be treated analytically there, using the Schur-Horn theorem [30][31]. Hopefully, one can study the critical points and zeros of $\mathcal{L}_D$ away from the complete mixed state by using an adjustment similiar to the method used in this paper. Instead of $\hat{n}$, one considers the flag formed by the eigenspaces of ρ. Such a flag can be made to vary continuously by applying a skew-Hermitian operator: its tangent space is a subspace of the Lie algebra $\mathfrak{su}(n)$. It is reasonable to assume that one can achieve an adjustment expression on the tangent space that preserves critical points and zeros.

Appendix A: Derivation of the Bloch vector ODE

A quantum density operator ρ is a trace-one, positive semi-definite operator. On an $n = 2$ Hilbert space, we can write:

$$\rho = \frac{1}{2}\left(I_2 + \sum_{j=x,y,z} n_j \sigma_j\right), \tag{A1}$$

where σ_j are the Pauli matrices:

$$\sigma_x = \begin{pmatrix} 0 & 1 \\ 1 & 0 \end{pmatrix}, \quad \sigma_y = \begin{pmatrix} 0 & -i \\ i & 0 \end{pmatrix}, \quad \sigma_z = \begin{pmatrix} 1 & 0 \\ 0 & -1 \end{pmatrix}, \tag{A2}$$

which obey the following relations:

$$[\sigma_j, \sigma_k] = 2i\epsilon_{jkl}\sigma_l \tag{A3}$$

$$\{\sigma_j, \sigma_k\} = 2\delta_{jk} I_2. \tag{A4}$$

It can be checked that the purity $Tr(\rho^2)$ is equal to the magnitude of the Bloch vector $r := |\vec{n}|$. It can also be

shown that the eigenvalues of ρ are $\lambda_\pm := \frac{1\pm r}{2}$. Each unitary orbit $\{U\rho U^\dagger : U \in U(2)\}$ corresponds to one value of $r \in [0,1]$.

If for $r \neq 0$, we write $\hat{n} := \vec{n}/r$, the eigenvectors of ρ are $|\psi_\pm\rangle := \frac{\hat{n}_z \pm 1}{2}|0\rangle + \frac{\hat{n}_x + i\hat{n}_y}{2}|1\rangle$. It follows that the set $\{|\psi_+\rangle\}$ can be identified with the set $\{\hat{n}\}$, which of course is S^2.

Using the above identification, we can transform the Lindblad equation to an ODE on $\mathbb{R}^3$. If we set $H = h_0 I_2 + \frac{1}{2}\sum_j h_j \sigma_j$, the Hamiltonian piece becomes:

$$[-iH, \rho] = \frac{1}{4}\sum_{j,k} h_j n_k [-i\sigma_j, \sigma_k] = \frac{1}{2}\sum_{j,k} h_j n_k \epsilon_{jkl}\sigma_l \tag{A5}$$

$$= \frac{1}{2}\sum_l \left(\vec{h}\times\vec{n}\right)_l \sigma_l. \tag{A6}$$

We can assume the Lindblad operators are traceless, as any traced part can be absorbed into the Hamiltonian [12]. In this case, we can write $L_m = \sum_{j=x,y,z} l_{j,m}\sigma_j$, where $l_{j,m} \in \mathbb{C}$. We have:

$$\mathcal{L}_D(\frac{I_2}{2}) = \frac{1}{2}\sum_{j,k,m} l_{j,m}\bar{l}_{k,m}[\sigma_j, \sigma_k] = \sum_{j,k,m} l_{j,m}\bar{l}_{k,m} i\epsilon_{jkl}\sigma_l \tag{A7}$$

$$= \sum_l b_l \sigma_l, \tag{A8}$$

where

$$\vec{b} = i\sum_m \vec{l}_m \times \vec{\bar{l}}_m. \tag{A9}$$

If all Lindblad operators are Hermitian, $\vec{b}$ vanishes. This is known as the unital case.

We also have:

$$\mathcal{L}_D(\sum_l \frac{n_l\sigma_l}{2}) = \sum_{j,k,l,m} l_{j,m}\bar{l}_{k,m}\frac{n_l}{4}(2\sigma_j\sigma_l\sigma_k - \sigma_k\sigma_j\sigma_l - \sigma_l\sigma_k\sigma_j) \tag{A10}$$

$$= \frac{1}{4}\sum_{j,k,l,m} l_{j,m}\bar{l}_{k,m} n_l(\delta_{jl}\sigma_k + \delta_{kl}\sigma_j - 2\delta_{jk}\sigma_l) \tag{A11}$$

$$= \frac{1}{2}\sum_{j,l,m} \frac{l_{l,m}\bar{l}_{j,m} + l_{j,m}\bar{l}_{l,m}}{2} n_l\sigma_j - l_{j,m}\bar{l}_{j,m} n_l\sigma_l \tag{A12}$$

$$= \frac{1}{2}\sum_l (A\vec{n})_l \sigma_l - \mathrm{tr}(A) n_l \sigma_l, \tag{A13}$$

where A is the symmetric matrix

$$A := \frac{1}{2}\sum_m (\vec{l}_m\vec{\bar{l}}_m^T + \vec{\bar{l}}_m\vec{l}_m^T). \tag{A14}$$

Since $\frac{d}{dt}\rho = \frac{1}{2}\sum_j \frac{dn_j}{dt}\sigma_j$, we can combine these pieces into the following ODE:

$$\frac{d\vec{n}}{dt} = \vec{b} + \vec{h}\times\vec{n} + (A - \mathrm{tr}(A))\vec{n}. \tag{A15}$$

Appendix B: Parameter conditions

Since A is a symmetric matrix, it has a natural orthonormal basis. In this basis, we have six system parameters: the eigenvalues $\{a_j\}$ of A and the elements $\{b_j\}$ of $\vec{b}$, with $j = 1,2,3$. These six parameters must obey two inequalities.

Consider the matrix $A_* = \sum_m \vec{l}_m\vec{\bar{l}}_m^T$. A_* is the sum of positive semi-definite matrice, and so itself must be positive semi-definite. Moreover, its real part, which equals A, must be positive semi-definite, so we have our first inequality:

$$a_j \geq 0 \tag{B1}$$

Now the imaginary part of A_* relates to $\vec{b}$: $b_1 = i(l_2\bar{l}_3 - l_3\bar{l}_2) = 2\,\mathrm{Im}(A_*)_{32}$ etc. If we write A_* in the natural basis of A, and take its determinant, we get:

$$\det(A_*) = a_1a_2a_3 - \frac{1}{4}(a_1b_1^2 + a_2b_2^2 + a_3b_3^2). \tag{B2}$$

Since the determinant of a positive semi-definite matrix must be non-negative, we recover the second inequality:

$$\vec{b}^T A\vec{b} \leq 4\det(A). \tag{B3}$$

Appendix C: Interpretation of Parameters

Let us consider (A15) with $\vec{h}$ set to zero. Because A is symmetric and positive semi-definite, it can be decomposed into $A = O^T A_d O$, where O is an orthogonal matrix and A_d is a diagonal matrix with entries $a_1 \geq a_2 \geq a_3 \geq 0$. If the eigenvalues a_j are distinct, there are three unique orthogonal axes in $\mathbb{R}^3$ which we call the *damping axes*, since the solution to (A15), if $\vec{b} = 0$, is

$$\vec{n}(t) = O^T \begin{pmatrix} e^{-(a_2+a_3)t} & 0 & 0 \\ 0 & e^{-(a_1+a_3)t} & 0 \\ 0 & 0 & e^{-(a_1+a_2)t} \end{pmatrix} O. \tag{C1}$$

Correspondingly, we have three damping rates: $r_1 = a_2 + a_3$, $r_2 = a_1 + a_3$ and $r_3 = a_1 + a_2$. If there is a double or triple eigenvalue, the axes are no longer unique due to symmetry. Nevertheless, a choice of damping axes can always be made (although damping does not occur in one direction if $a_2 = a_3 = 0$).

In the Hilbert space, these three damping axes correspond to a sextet of quantum states. If we choose the axis corresponding to the largest eigenvalue a_1, it defines two

orthonormal states $|\alpha_{1+}\rangle$ and $|\alpha_{1-}\rangle$. The remaining four states can be written $|\alpha_{j\pm}\rangle = \frac{1}{\sqrt{2}}(|\alpha_{1+}\rangle + e^{i(\theta_0+\theta_{j\pm})}|\alpha_{1-}\rangle)$ where $\theta_{2\pm} = 0, \pi$ and $\theta_{3\pm} = \frac{\pi}{2}, \frac{3\pi}{2}$. The so-called phase-damping channel corresponds to the case where $|\alpha_{1\pm}\rangle$ are the energy eigenstates, $\vec{b} = 0$, and $a_2 = a_3 = 0$. We can infer then that a general Lindblad super-operator includes three phase-damping channels. The phases in question are not necessarily phases with respect to the energy eigenstates, as the interaction with the environment may favor other states.

We call $\vec{b}$ the *damping-bias vector*, because it biases the damping in a certain direction. When it is zero and $a_2 > 0$, the unbiased system relaxes to the point $\vec{n} = 0$, which is the completely mixed state (if $a_2 = 0$, only two components relax to zero, while the other does not change). Such a process corresponds to a so-called unital Lindblad super-operator, where $\mathcal{L}_D(\rho) = 0$. If the damping is biased however, the system relaxes to a point where the coordinates with respect to the decay axes are $\frac{b_j}{r_j}$. Note that the inequality (B3) ensures that $b_j = 0$ if $r_j = 0$, and that the relaxation point always falls inside the Bloch ball.

The so-called amplitude-damping occurs when $a_1 = a_2 > a_3 = 0 = b_1 = b_2$ and $b_3 = r_3 = 2a_1$ (assuming $|\alpha_{1\pm}\rangle$ are the energy eigenstates). The system relaxes to the point $\vec{n} = (1, 0, 0)$ which is the ground energy eigenstate. In this example, the bias is saturated in some sense because the relaxation point is on the Bloch sphere; the dissipation cannot be any more biased in that direction. This type of dissipation is also seen in the cooling problem [17], where spontaneous emission of photons causes the system to relax to the ground state. One can extend this to model both absorption and emission of photons in a reservoir at non-zero temperature by having two amplitude-damping channels: one to the ground state $|g\rangle$, and one to the excited state $|e\rangle$. In this case, we have $-r_3 < b_3 < r_3$, so that the system relaxes to a mixture $\rho = \frac{1+b_3}{2}|g\rangle\langle g| + \frac{1-b_3}{2}|e\rangle\langle e|$.

ACKNOWLEDGMENTS

P.R. has been supported by the National Science Foundation and the DFG grant HE 1858/13-1 from the German Research Foundation (DFG). A.M.B. is supported by the National Science Foundation. C.R. is supported by the Natural Science and Engineering Research Council of Canada.

[1] M. Shapiro and P. Brumer. Laser control of product quantum state populations in unimolecular reactions. *J. Phys. Chem.*, 84(7):4103, 1986.

[2] D. J. Tannor and S. A. Rice. Control of selectivity of chemical reaction via control of wave packet evolution. *J. Chem. Phys.*, 83(10):5013, 1985.

[3] R. R. Ernst, G. Bodenhausen, and A. Wokaun. *Principles of Nuclear Magnetic Resonance in One and Two Dimensions*. Clarendon, Oxford, 1987.

[4] C. Rangan and P. H. Bucksbaum. Optimally shaped terahertz pulses for phase retrieval in a Rydberg-atom data register. *Phys. Rev. A*, 64:033417, 2001.

[5] J. P. Palao and R. Kosloff. Quantum computing by an optimal control algorithm for unitary transformations. *Phys. Rev. Lett.*, 89(18):188301, 2002.

[6] H. Mabuchi and N. Khaneja. Principles and applications of control in quantum systems. *Int J. Robust and Nonlinear Control*, 15:647 – 667, 2005.

[7] Brif, Chakrabarti, and H. Rabitz. Control of quantum phenomena: past, present and future. *New J. Phys.*, 12(5):075008, 2010.

[8] D. Dong and I. Petersen. Quantum control theory and applications: a survey. *IET Control theory and applications*, 4(12):2651 –2671, 2011.

[9] C. Altafini and F. Ticozzi. Modeling and control of quantum systems: an introduction. *IEEE Transactions on Automatic Control*, 57:1898 – 1917, 2012.

[10] G. Lindblad. On the generators of quantum dynamical semigroups. *Comm. Math. Phys.*, 48:119, 1976.

[11] V. Gorini, A. Kossakowski, and E.C.G. Sudarshan. Completely positive dynamical semigroups of N-level systems. *J. Math. Phys.*, 17(5):821, 1976.

[12] H.-P. Breuer and F. Petruccione. *The Theory of Open Quantum Systems*. Oxford University Press, 2007.

[13] S. Lloyd and L. Viola. Engineering quantum dynamics. *Phys. Rev. A*, 65:010101, 2001.

[14] D. Bacon et al. Universal simulation of Markovian quantum dynamics. *Phys. Rev. A*, 64:062302, 2001.

[15] J.T. Barreiro et al. An open-system quantum simulator with trapped ions. *Nature*, 470:486, 2011.

[16] D. J. Tannor and A. Bartana. On the interplay of control fields and spontaneous emission in laser cooling. *J. Phys. Chem. A*, 103:10359, 1999.

[17] S. E. Sklarz, D. J. Tannor, and N. Khaneja. Optimal control of quantum dissipative dynamics: Analytic solution for cooling the three-level Λ system. *Phys. Rev. A*, 69:053408, 2004.

[18] S. G. Schirmer, T. Zhang, and J.V. Leahy. Orbits of quantum states and geometry of Bloch vectors for N-level systems. *J. Phys. A*, 37:1389, 2004.

[19] N. Khaneja, S.J. Glaser, and R.W. Brockett. Sub-riemannian geometry and time optimal control of three spin systems: Quantum gates and coherence transfer. *Phys. Rev. A*, 65:032301, 2002.

[20] S. Schirmer and X. Wang. Stabilizing open quantum systems by markovian reservoir engineering. *Physical Review A*, 81:062306, 2010.

[21] C. Altafini. Feedback stabilization of isospectral control systems on complex flag manifolds: Application to quantum ensembles. *IEEE Trans. Aut. Cont.*, 52(11):2019, 2007.

[22] I. Bengtsson and K. Zyczkowski. *Geometry of Quantum States*. Cambridge University Press, 2006.

[23] P. Rooney, A.M. Bloch, and C. Rangan. Decoher-

ence control and purification of two-dimensional quantum density matrices under Lindblad dissipation. 2012. arXiv:1201.0399v1 [quant-ph].

[24] H. Yuan. Reachable set of open quantum dynamics for a single spin in markovian environment. *Automatica*, 49:955–959, 2013.

[25] J. Preskill. Lecture notes on quantum computation. `http://www.theory.caltech.edu/people/preskill/ph229/notes/chap3.pdf`.

[26] P. Rooney, A.M. Bloch, and C. Rangan. Flag-based control of orbit dynamics for quantum Lindblad systems. 2016 (in press). arXiv:1602.06353 [quant-ph].

[27] J. Stewart. *Multivariate Calculus, 8th ed.* Brooks Cole, 2015.

[28] S. Lang. *Introduction to Differential Manifolds, 2nd ed.* Springer-Verlag, 2002.

[29] E. Celledoni, H. Marthinsen, and B. Owren. An introduction to Lie group integrators - basics, new developments and applications. *J. Comp. Phys.*, 257:1040 – 1061, 2014.

[30] I. Schur. Über eine Klasse von Mittelbildungen mit Anwendungen auf die Determinantentheorie. *Sitzungsber. Berl. Math. Ges.*, 22:9, 1923.

[31] A. Horn. Doubly stochastic matrices and the diagonal of a rotation matrix. *Am. J. Math.*, 76:620, 1954.